Dynamics of a Space Multi-pointing Stewart System Using the New Form of Kane's Method

By Quan HU,[1*] Fei LIU,[1] and Yao ZHANG[1]

[1)] *School of Aerospace Engineering, Beijing Institute of Technology, Beijing, China*

(Received June 21st, 2017)

This paper addresses the dynamic modeling for the space multi-pointing Stewart system (SMSS). The main feature of the SMSS is that a six-degrees-of-freedom (6 DOFs) Stewart mechanism is adopted to connect the central hub of the on-orbit satellite and the optical payload, so that the pointing of the payload can be precisely controlled by the active actuators in the Stewart mechanism, rather than by the attitude controls in the satellite only. To evaluate SMSS's dynamic characteristics and design its control systems, a comprehensive dynamic model is indispensable. Since the Stewart mechanism brings closed-loop motion constraints to SMSS, the formulation of the equations of motion is performed in two steps. Firstly, the motion constraints are released so that the Kane's method in matrix form can be used to derive the governing equations of the unconstrained system. Then, to avoid introducing unknown multipliers, the new form of Kane's method is applied to handle the closed-loop motion constraints. The obtained equations of motion incorporate all the mass parameters of the bodies in SMSS, and can be directly used for control synthesis.

Key Words: Active Multi-pointing System; Stewart Platform; Kane's Equation; Reduced Model.

Nomenclature

$\boldsymbol{\Delta}_j$	:	modal selection matrix
$\boldsymbol{F}^A$	:	generalized active force
$\boldsymbol{F}^I$	:	generalized inertia force
$\vec{\boldsymbol{F}}_s$	:	the s th external force
$\vec{\Gamma}_j, \boldsymbol{\Gamma}_j$	:	vector characterizing the joint h_j
K	:	total degrees of freedom (DOFs)
$\boldsymbol{M}$	:	inertia matrix
$\vec{\boldsymbol{N}}_l$	:	the l th external torque
n	:	body number in the multibody system
$\boldsymbol{\tau}$	:	modal coordinate
$\vec{t}_j, \boldsymbol{t}_j$	:	the translation at the prismatic joint
$\vec{\boldsymbol{T}}$	:	translational modal vector
$\boldsymbol{u}$	:	generalized speeds
$\vec{\boldsymbol{u}}$	:	elastic displacement
$\vec{\boldsymbol{v}}$	:	velocity
${}^p\vec{\boldsymbol{v}}$	:	partial velocity
${}^p\vec{\boldsymbol{\omega}}$	:	partial angular velocity

Subscripts

D	:	dependent
r	:	rigid
f	:	flexible
i	:	number for the generalized speeds
I	:	independent
j	:	body number
mj	:	element mass in body B_j
p	:	partial
r	:	rigid
t	:	nonlinear component

1. Introduction

The Stewart platform is a six-degrees-of-freedom (6 DOFs) mechanism composed of two rigid bodies connected by six extensible struts.[1-3)] It has been wildly used for passive vibration isolation in imaging spacecrafts.[4-6)] By introducing active actuators to the extensible struts, the Stewart platform can also be used for attitude maneuver of the payload to realize the precise multi-pointing. In this work, we focus on the dynamics modeling issue related to such application.

The considered space multi-pointing Stewart system (SMSS) is constituted of a rigid central hub, two solar panels, a Stewart mechanism and a flexible payload (such as a long mirror cylinder or a space truss). As Fig. 1 shows, it is a typical multibody system subject to nonholonomic constraints. In fact, much research have been performed on the dynamics of the Stewart platform by employing the Lagrange equation,[7)] Newton–Euler method,[8,9)] and Kane's equation.[3)] The Lagrange formulation involves the partial derivatives of the Lagrangian, so a large amount of symbolic computation is required. Furthermore, the multipliers are adopted to describe the constraints in this formulation, which increases the dimension of the system and leads to difficulty for controller design. When using the Newton–Euler method, one have to eliminate (or calculate) the interaction forces between each body; and yet, this procedure also related with tedious derivations for the unknown forces[8,9)]. The above issues could be avoided in the Kane's method, but the unknown multipliers are also introduced for the nonholonomic constraints.[3)]

In this work, the new form of Kane's method is adopted to obtain the equations of motion of the SMSS without introducing multipliers.[10)] The equivalent unconstrained system is demonstrated in Fig. 2, whose governing equation is firstly formulated by the Kane's equation in matrix form. Then, the new form of Kane's equation is used to handle the nonholonomic constraints, then the equations of motion are finally reduced to a minimum order. The obtained equations of motion is quite suitable for controller design.

2. System Description

As it is shown in Fig. 1, the Stewart platform connects the payload and the central hub to precisely control their relative translation and rotation. It is composed of six extensible struts. Each strut connect to the upper and lower platform by a spherical joint or a Hooke joint respectively. Besides, an active prismatic joint is embedded in each strut to enable the change of its length. The Stewart mechanism brings five closed-loop constraints to the system, which makes it a typical multibody system with nonholonomic constraints. To establish its governing equation, we firstly derive the equations of motion of the equivalent unconstrained system, and then model the nonholonomic constraints specially.

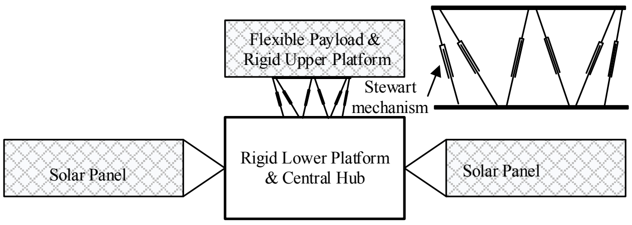

Fig. 1. Space Multi-pointing Stewart System.

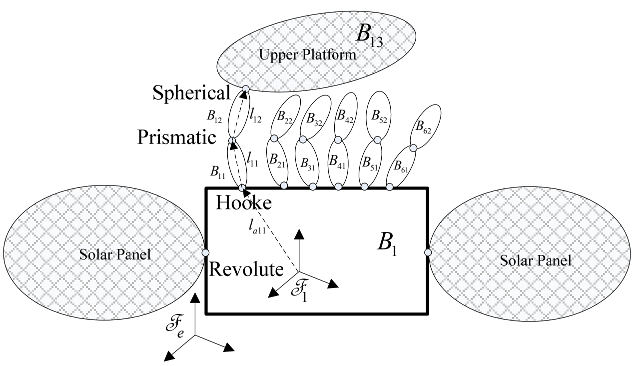

Fig. 2. The equivalent system without motion constants.

The equivalent unconstrained system is obtained by introducing five corresponding cut points to remove the closed-loops, as Fig. 2 shows. This treatment leads to a multibody system in tree topology. The number of body is 16, since each strut is viewed as two links connected by a prismatic joint. However, for sake of generality, we suppose there are n rigid bodies and n joints. The n bodies can be numbered as shown in Fig. 2 and each joint has the same number with its outboard body. A body fixed frame $\mathcal{F}_j$ is attached to B_j ($j=1,2,...,n$), while the inertial frame is denoted by $\mathcal{F}_e$.

The generalized speeds for the unconstrained system can be chosen as

$$\boldsymbol{u} = [\boldsymbol{u}_1^T, \boldsymbol{u}_2^T, ...\boldsymbol{u}_n^T]^T \tag{1}$$

where $\boldsymbol{u}_j$ is the generalized speeds for B_j and the superscript "T" denotes the transpose of a matrix. $\boldsymbol{u}_j$ describes the relative motion between B_j and its inboard body $B_{c(j)}$. If B_j is flexible, the assumed mode method is adopted to describe the structural vibration. In this case, we define $\boldsymbol{u}_i = [\boldsymbol{u}_i^{rT}, \boldsymbol{\tau}_i^T]^T$. Thus the total DOFs of the unconstrained system is given by

$$K = \sum_{i=1}^{n} \dim(\boldsymbol{u}_i) \tag{2}$$

3. Equations of Motion of the Unconstrained System

In this section, we formulate the equations of motion by the Kane's equation in matrix form. The notions "*partial velocity matrix*" and "*partial angular velocity matrix*", [10-12] would be first introduced, so that each body's contribution to the generalized inertia force would be expressed by a same equation. Thus, the system inertia matrix and the nonlinear forces can be directly extracted by simply add up the contributions of each body. Then, the kinematics of the Hooke, prismatic, and spherical joints will be written in a compatible manner with the dynamics equation.

3.1 Kane's Equation in Matrix Form

The equations of motion of a multibody system in tree topology can be written as

$$\boldsymbol{F}_i^I + \boldsymbol{F}_i^A = \boldsymbol{0} \quad (i=1,2,\cdots n) \tag{3}$$

where $\boldsymbol{F}_i^I$ and $\boldsymbol{F}_i^A$ are the generalized inertia force and generalized active force with respect to $\boldsymbol{u}_i$. $\boldsymbol{F}_i^I$ is calculated by

$$\boldsymbol{F}_i^I = -\sum_{j=1}^{n} \int_{Bj} {}^p_i\vec{\boldsymbol{v}}_{mj} \cdot \dot{\vec{\boldsymbol{v}}}_{mj} dm \quad (i=1,2,\cdots n) \tag{4}$$

where $\vec{\boldsymbol{v}}_{mj}$ is the inertial velocity of dm and ${}^p_i\vec{\boldsymbol{v}}_{mj}$ is the partial velocity of the element mass dm corresponding to the i th generalized speed $\boldsymbol{u}_i$. It is defined by the fact that, $\vec{\boldsymbol{v}}_{mj}$ is a linear combination of $\boldsymbol{u}_i$,

$$\vec{\boldsymbol{v}}_{mj} = \sum_{i=1}^{n} {}^p_i\vec{\boldsymbol{v}}_{mj}\boldsymbol{u}_i + \vec{\boldsymbol{v}}_{mjt} \tag{5}$$

The linear coefficients in Eq. (5) are defined as the partial velocity; whereas $\vec{\boldsymbol{v}}_{mjt}$ is a function of the generalized coordinates and time.

For the generalized active force $\boldsymbol{F}_i^A$, we assume that S active forces and L active torques are exerted on the unconstrained system. Then, we have

$$\boldsymbol{F}_i^A = \sum_{s=1}^{S} {}^p_i\vec{\boldsymbol{v}}_s \vec{\boldsymbol{F}}_s + \sum_{l=1}^{L} {}^p_i\vec{\boldsymbol{\omega}}_l \vec{\boldsymbol{N}}_l \tag{6}$$

where ${}^p_i\vec{\boldsymbol{v}}_s$ is the i th partial velocity of the point where force $\vec{\boldsymbol{F}}_s$ is exerted; ${}^p_i\vec{\boldsymbol{\omega}}_l$ is the partial angular velocity of the place where $\vec{\boldsymbol{N}}_l$ is exerted.

The formulation of $\boldsymbol{F}_i^A$ is quite straightforward, but more efforts are required to have the explicit expression of $\boldsymbol{F}_i^I$. In what follows, the integration of $\boldsymbol{F}_i^I$ would be fully expanded.

3.2 Generalized Inertia Force

Consider the two adjacent bodies in a multibody system (Fig. 3), $B_{c(j)}$ is the inboard body of B_j. They are connected by joint h_j, whose DOFs can be 1~6. To obtain a universal derivations, we assume that both $B_{c(j)}$ and B_j are flexible.

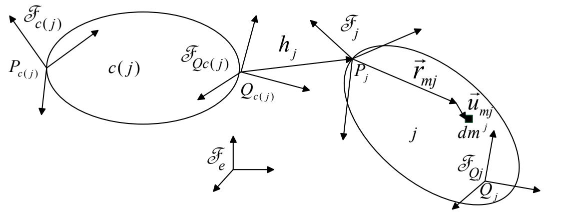

Fig. 3. Two adjacent bodies in an unconstrained multibody system.

The inertial velocity and inertial angular velocity of $\mathcal{F}_j$ can also be expressed as the linear combination of $\boldsymbol{u}_i$,

$$\vec{\boldsymbol{v}}_j = \sum_{i=1}^{n} {}_i^p\vec{\boldsymbol{v}}_j \boldsymbol{u}_i + \vec{\boldsymbol{v}}_{jt} \tag{7}$$

$$\vec{\boldsymbol{\omega}}_j = \sum_{i=1}^{n} {}_i^p\vec{\boldsymbol{\omega}}_j \boldsymbol{u}_i + \vec{\boldsymbol{\omega}}_{jt} \tag{8}$$

where ${}_i^p\vec{\boldsymbol{v}}_j$ and ${}_i^p\vec{\boldsymbol{\omega}}_j$ are the i th partial velocity and partial angular velocity of $\mathcal{F}_j$, respectively. $\vec{\boldsymbol{v}}_{jt}$ and $\vec{\boldsymbol{\omega}}_{jt}$ have similar definitions with $\vec{\boldsymbol{v}}_{mjt}$.

To simplify the formulation and clarify each body's the contribution to the equations of motion in the system, we define

$$\begin{cases} {}^p\vec{\boldsymbol{v}}_{mj} = [{}_1^p\vec{\boldsymbol{v}}_{mj} \ \ {}_2^p\vec{\boldsymbol{v}}_{mj} \cdots \ {}_n^p\vec{\boldsymbol{v}}_{mj}] \\ {}^p\vec{\boldsymbol{\omega}}_{mj} = [{}_1^p\vec{\boldsymbol{\omega}}_{mj} \ \ {}_2^p\vec{\boldsymbol{\omega}}_{mj} \cdots {}_n^p\vec{\boldsymbol{\omega}}_{mj}] \end{cases} \tag{9}$$

where ${}^p\vec{\boldsymbol{v}}_{mj}$ is termed as the *partial velocity matrix*, and ${}^p\vec{\boldsymbol{\omega}}_{mj}$ is the *partial angular velocity matrix* of *dm.* According to Eq. (5), we have

$$\vec{\boldsymbol{v}}_{mj} = {}^p\vec{\boldsymbol{v}}_{mj}\boldsymbol{u} + \vec{\boldsymbol{v}}_{mjt} \tag{10}$$

Moreover, the generalized inertia forces related with B_j can be stacked together and expressed as

$$\begin{aligned} \boldsymbol{F}_j^I &= [(\boldsymbol{F}_{j1}^I)^T,...,(\boldsymbol{F}_{jn}^I)^T]^T \\ &= -\int_{Bj} {}^p\vec{\boldsymbol{v}}_{mj} \cdot \dot{\vec{\boldsymbol{v}}}_{mj} dm \end{aligned} \tag{11}$$

Similarly, the partial velocity matrix ${}^p\vec{\boldsymbol{v}}_j$ and partial angular velocity matrix ${}^p\vec{\boldsymbol{\omega}}_j$ of $\mathcal{F}_j$ are written as

$$\begin{cases} {}^p\vec{\boldsymbol{v}}_j = [{}_1^p\vec{\boldsymbol{v}}_j \ \ {}_2^p\vec{\boldsymbol{v}}_j \cdots \ {}_n^p\vec{\boldsymbol{v}}_j] \\ {}^p\vec{\boldsymbol{\omega}}_j = [{}_1^p\vec{\boldsymbol{\omega}}_j \ \ {}_2^p\vec{\boldsymbol{\omega}}_j \cdots {}_n^p\vec{\boldsymbol{\omega}}_j] \end{cases} \tag{12}$$

Then, the inertial velocity and inertial angular velocity in Eqs. (7) and (8) become

$$\begin{cases} \vec{\boldsymbol{v}}_j = {}^p\vec{\boldsymbol{v}}_j\boldsymbol{u} + \vec{\boldsymbol{v}}_{jt} \\ \vec{\boldsymbol{\omega}}_j = {}^p\vec{\boldsymbol{\omega}}_j\boldsymbol{u} + \vec{\boldsymbol{\omega}}_{jt} \end{cases} \tag{13}$$

Furthermore, the *modal selection matrix* for B_j is defined to make the following equation always satisfied,

$$\dot{\boldsymbol{\tau}}_j = \boldsymbol{\Delta}_j\boldsymbol{u} \, , \, \boldsymbol{\Delta}_j \in \mathbb{R}^{K_j^f \times K} \tag{14}$$

where K_j^f is the modes number for the flexible body B_j. Obviously, $\boldsymbol{\Delta}_j$ has the following form,

$$\boldsymbol{\Delta}_j = [\boldsymbol{0},...,\boldsymbol{0}, \boldsymbol{I}_{K^f \times K^f}, \boldsymbol{0},...,\boldsymbol{0}] \tag{15}$$

where $\boldsymbol{I}$ and $\boldsymbol{0}$ are the unity matrix and null matrix with appropriate dimension, respectively.

The inertial velocity of *dm* can be written as

$$\vec{\boldsymbol{v}}_{mj} = \vec{\boldsymbol{v}}_j + \vec{\boldsymbol{\omega}}_j \times (\vec{\boldsymbol{r}}_{mj} + \vec{\boldsymbol{u}}_{mj}) + \dot{\vec{\boldsymbol{u}}}_{mj} \tag{16}$$

where $\vec{\boldsymbol{r}}_{mj}$ is the position of *dm* relative to the origin of $\mathcal{F}_j$ in the undeformed state. $\vec{\boldsymbol{u}}_{mj}$ is the elastic displacement of *dm*, discretized by

$$\vec{\boldsymbol{u}}_{mj} = \vec{\boldsymbol{T}}_{mj}\boldsymbol{\tau}_j \tag{17}$$

Substituting Eqs. (13), (14) and (17) into Eq. (16) yields

$$\begin{aligned} \vec{\boldsymbol{v}}_{mj} = &({}^p\vec{\boldsymbol{v}}_j + {}^p\vec{\boldsymbol{\omega}}_j \times (\vec{\boldsymbol{r}}_{mj} + \vec{\boldsymbol{u}}_{mj}) + \vec{\boldsymbol{T}}_{mj}\boldsymbol{\Delta}_j)\boldsymbol{u} \\ &+ (\vec{\boldsymbol{v}}_{jt} + \vec{\boldsymbol{\omega}}_{jt} \times (\vec{\boldsymbol{r}}_{mj} + \vec{\boldsymbol{u}}_{mj})) \end{aligned} \tag{18}$$

Comparing Eq. (10) with Eq. (18), the relation for the partial velocity is obtained,

$${}^p\vec{\boldsymbol{v}}_{mj} = {}^p\vec{\boldsymbol{v}}_j + {}^p\vec{\boldsymbol{\omega}}_j \times (\vec{\boldsymbol{r}}_{mj} + \vec{\boldsymbol{u}}_{mj}) + \vec{\boldsymbol{T}}_{mj}\boldsymbol{\Delta}_j \tag{19}$$

Time derivative of Eq. (16) leads to the inertial acceleration of *dm*,

$$\begin{aligned} \dot{\vec{\boldsymbol{v}}}_{mj} = &\dot{\vec{\boldsymbol{v}}}_j + \dot{\vec{\boldsymbol{\omega}}}_j \times (\vec{\boldsymbol{r}}_{mj} + \vec{\boldsymbol{u}}_{mj}) + \vec{\boldsymbol{T}}_{mj}\ddot{\vec{\boldsymbol{\tau}}}_j \\ &+ 2\vec{\boldsymbol{\omega}}_j \times \dot{\vec{\boldsymbol{u}}}_{mj} + \vec{\boldsymbol{\omega}}_j \times \vec{\boldsymbol{\omega}}_j \times (\vec{\boldsymbol{r}}_{mj} + \vec{\boldsymbol{u}}_{mj}) \end{aligned} \tag{20}$$

Substituting Eqs. (19) and (20) into Eq. (11) and perform the integration on B_j, we obtain the generalized inertia forces of B_j as

$$\begin{aligned} \boldsymbol{F}_j^I = &-{}^p\vec{\boldsymbol{v}}_j \cdot [m_j\dot{\vec{\boldsymbol{v}}}_j - \vec{\boldsymbol{S}}_j \times \dot{\vec{\boldsymbol{\omega}}}_j + \vec{\boldsymbol{P}}_j\ddot{\boldsymbol{\tau}}_j + 2\vec{\boldsymbol{\omega}}_j \times \vec{\boldsymbol{P}}_j\dot{\tau}_j + \vec{\boldsymbol{\omega}}_j \times \vec{\boldsymbol{\omega}}_j \times \vec{\boldsymbol{S}}_j] \\ &- {}^p\vec{\boldsymbol{\omega}}_j \cdot [\vec{\boldsymbol{S}}_j \times \dot{\vec{\boldsymbol{v}}}_j + \boldsymbol{J}_j\dot{\vec{\boldsymbol{\omega}}}_j + \vec{H}_j\ddot{\boldsymbol{\tau}}_j + 2\vec{\boldsymbol{H}}_{\omega j}\dot{\boldsymbol{\tau}}_j + \vec{\boldsymbol{\omega}}_j \times \boldsymbol{J} \cdot \vec{\boldsymbol{\omega}}_j] \\ &- \boldsymbol{\Delta}_j^T[\vec{\boldsymbol{P}}_j \cdot \dot{\vec{\boldsymbol{v}}}_j + \vec{\boldsymbol{H}}_j \cdot \dot{\vec{\boldsymbol{\omega}}}_j + \boldsymbol{E}_j\ddot{\boldsymbol{\tau}}_j + 2\vec{\boldsymbol{F}}_{\omega j}\dot{\boldsymbol{\tau}}_j + \vec{\boldsymbol{F}}_{\omega\omega j}] \end{aligned} \tag{21}$$

where the details of the integrals m_j, $\vec{\boldsymbol{S}}_j$, $\boldsymbol{J}_j$, $\vec{\boldsymbol{P}}_j$, $\vec{\boldsymbol{H}}_j$, $\vec{\boldsymbol{H}}_{\omega j}$, $\boldsymbol{E}_j$, $\vec{\boldsymbol{F}}_{\omega j}$, and $\vec{\boldsymbol{F}}_{\omega\omega j}$ are given in the Appendix.

3.3 System Equations of Motion

Observing Eq. (21), $\boldsymbol{F}_j^I$ can be divided into two groups: the one consists of all the terms that are explicit in the derivatives of generalized speeds, and the other does not:

$$\boldsymbol{F}_j^I = -\boldsymbol{F}_{j0}^I - \boldsymbol{F}_{jt}^I \tag{22}$$

where the one linear in $\dot{\boldsymbol{u}}$ can be written in a compact form,

$$\boldsymbol{F}_{j0}^I = \boldsymbol{M}_j\dot{\boldsymbol{u}} \tag{23}$$

where $\boldsymbol{M}_j \in \mathbb{R}^{K \times K}$ is B_j's contribution to the system inertia matrix, calculated by

$$\begin{aligned} \boldsymbol{M}_j = &{}^p\vec{\boldsymbol{v}}_j \cdot [m_j{}^p\vec{\boldsymbol{v}}_j - \vec{\boldsymbol{S}}_j \times {}^p\vec{\boldsymbol{\omega}}_j + \vec{\boldsymbol{P}}_j\boldsymbol{\Delta}_j] \\ &+ {}^p\vec{\boldsymbol{\omega}}_j \cdot [\vec{\boldsymbol{S}}_j \times {}^p\vec{\boldsymbol{v}}_j + \boldsymbol{J}_j{}^p\vec{\boldsymbol{\omega}}_j + \vec{\boldsymbol{H}}_j\boldsymbol{\Delta}_j] \\ &+ \boldsymbol{\Delta}_j^T[\vec{\boldsymbol{P}}_j \cdot {}^p\vec{\boldsymbol{v}}_j + \vec{\boldsymbol{H}}_j \cdot {}^p\vec{\boldsymbol{\omega}}_j + \boldsymbol{E}_j\boldsymbol{\Delta}_j] \end{aligned} \tag{24}$$

$\boldsymbol{F}_{jt}^I$ in Eq. (22) is the contribution of B_j to the system nonlinear generalized inertia force, expressed by

$$\begin{aligned} \boldsymbol{F}_{jt}^I = &{}^p\vec{\boldsymbol{v}}_j \cdot [m_j\dot{\vec{\boldsymbol{v}}}_{jt} - \vec{\boldsymbol{S}}_j \times \dot{\vec{\boldsymbol{\omega}}}_{jt} + 2\vec{\boldsymbol{\omega}}_j \times \vec{\boldsymbol{P}}_j\dot{\boldsymbol{\tau}}_j + \vec{\boldsymbol{\omega}}_j \times \vec{\boldsymbol{\omega}}_j \times \vec{\boldsymbol{S}}_j] \\ &+ {}^p\vec{\boldsymbol{\omega}}_j \cdot [\vec{\boldsymbol{S}}_j \times \dot{\vec{\boldsymbol{v}}}_{jt} + \boldsymbol{J}_j\dot{\vec{\boldsymbol{\omega}}}_{jt} + 2\vec{\boldsymbol{H}}_{\omega j}\dot{\boldsymbol{\tau}}_j + \vec{\boldsymbol{\omega}}_j \times \boldsymbol{J} \cdot \vec{\boldsymbol{\omega}}_j] \\ &+ \boldsymbol{\Delta}_j^T[\vec{\boldsymbol{P}}_j \cdot \dot{\vec{\boldsymbol{v}}}_{jt} + \vec{\boldsymbol{H}}_j \cdot \dot{\vec{\boldsymbol{\omega}}}_{jt} + 2\vec{\boldsymbol{F}}_{\omega j}\dot{\boldsymbol{\tau}}_j + \vec{\boldsymbol{F}}_{\omega\omega j}] \end{aligned} \tag{25}$$

Since the system generalized inertia force can be calculated by

$$\boldsymbol{F}^I = \sum\nolimits_{j=1}^{n} \boldsymbol{F}_j^I \tag{26}$$

the inertia matrix and the nonlinear terms of the entire system can be obtained as

$$\boldsymbol{M} = \sum_{j=1}^{N} \boldsymbol{M}_j \quad , \quad \boldsymbol{F}_t^I = \sum_{j=1}^{N} \boldsymbol{F}_{jt}^I \tag{27}$$

Finally, the equations of motion of the unconstrained system are written as

$$\boldsymbol{M}\dot{\boldsymbol{u}} + \boldsymbol{F}_t^I = \boldsymbol{F}^A \tag{28}$$

where $\boldsymbol{F}^A$ is the generalized active forces rearranged by

$$\boldsymbol{F}^A = [(\boldsymbol{F}_1^A)^T, ..., (\boldsymbol{F}_n^A)^T]^T \tag{29}$$

4. Kinematics of the Joints

In this section, the kinematic terms $\vec{\omega}_j$, ${}^p\vec{v}_j$, ${}^p\vec{\omega}_j$, $\dot{\vec{v}}_{jt}$ and $\dot{\vec{\omega}}_{jt}$, required in Eqs. (24) and (25), will be discussed for the joints in the SMSS. The recursive kinematic relations are specially developed to improve the modeling efficiency.

4.1 Revolute Joint

As shown in Fig. 2, the central hub and the solar panels are connected by the revolute joints. Denote the central hub by $\mathrm{B}_{c(j)}$ and the solar panel by B_j. Then, the recursive relationship between $\vec{\omega}_{c(j)}$ and $\vec{\omega}_j$ is written as

$$\vec{\omega}_j = \vec{\omega}_{c(j)} + \vec{\Gamma}_j \boldsymbol{u}_j \tag{30}$$

where $\vec{\Gamma}_j$ is the vector characterizing the direction of revolution; $\boldsymbol{u}_j$ is the relative rotational speed between $\mathrm{B}_{c(j)}$ and B_j. Equation (30) can be rewritten in a vectrix form

$$\vec{\omega}_j = \mathscr{F}_{c(j)}^T \boldsymbol{\omega}_{c(j)} + \mathscr{F}_j^T \boldsymbol{\Gamma}_j \boldsymbol{u}_j \tag{31}$$

where $\mathscr{F}_{c(j)}$ and $\mathscr{F}_j$ are the vectrices for frames $\mathcal{F}_{c(j)}$ and $\mathcal{F}_j$, respectively. The vectrix of $\mathcal{F}_j$ is given by $\mathscr{F}_j = [\vec{x}_j, \vec{y}_j, \vec{z}_j]^T$, where $\vec{x}_j$, $\vec{y}_j$, and $\vec{z}_j$ are the three unit orthogonal vectors of $\mathcal{F}_j$. Differentiating Eq. (31) with respect to time, we have

$$\dot{\vec{\omega}}_j = \mathscr{F}_{c(j)}^T \dot{\boldsymbol{\omega}}_{c(j)} + \mathscr{F}_j^T \boldsymbol{\Gamma}_j \dot{\boldsymbol{u}}_j + \mathscr{F}_j^T \tilde{\boldsymbol{\omega}}_j \boldsymbol{\Gamma}_j \boldsymbol{u}_j \tag{32}$$

Suppose $\boldsymbol{u}_j = \dot{\theta}_j$ is the x th element in the generalized speeds vector $\boldsymbol{u}$. Then, substituting $\vec{\omega}_{c(j)} = \mathscr{F}_{c(j)}^T \boldsymbol{\omega}_{c(j)} = {}^p\vec{\omega}_{c(j)} \boldsymbol{u} + \vec{\omega}_{c(j)t}$ into Eqs. (31) and (32) leads to the recursive relations for the partial angular velocity matrices and the nonlinear part of the angular accelerations, respectively,

$${}^p\vec{\omega}_j = {}^p\vec{\omega}_{c(j)} + [\boldsymbol{0}_{3\times1} \cdots \boldsymbol{0}_{3\times1} \underbrace{\vec{\Gamma}_j}_{x} \boldsymbol{0}_{3\times1} \cdots \boldsymbol{0}_{3\times1}] \quad , \quad {}^p\vec{\omega}_j \in \mathbb{R}^{3\times K} \tag{33}$$

$$\dot{\vec{\omega}}_{jt} = \dot{\vec{\omega}}_{c(j)t} + \mathscr{F}_j^T \tilde{\boldsymbol{\omega}}_j \boldsymbol{\Gamma}_j \boldsymbol{u}_j \tag{34}$$

where x indicates the position of $\vec{\Gamma}_j$ in the $3\times K$ matrix.

Similarly, the counterparts related with the velocities of $\mathrm{B}_{c(j)}$ and B_j can be obtained as

$${}^p\vec{v}_j = {}^p\vec{v}_{c(j)} - \mathscr{F}_{c(j)}^T \tilde{\boldsymbol{l}}_{c(j)} {}^p\vec{\omega}_{c(j)} \quad , \quad {}^p\vec{v}_j \in \mathbb{R}^{3\times K} \tag{35}$$

$$\dot{\vec{v}}_{jt} = \dot{\vec{v}}_{c(j)t} - \mathscr{F}_{c(j)}^T \tilde{\boldsymbol{l}}_{c(j)} \mathscr{F}_{c(j)} \dot{\vec{\omega}}_{c(j)t} + \mathscr{F}_{c(j)}^T \tilde{\boldsymbol{\omega}}_{c(j)} \tilde{\boldsymbol{\omega}}_{c(j)} \boldsymbol{l}_{c(j)} \tag{36}$$

where $\vec{\boldsymbol{l}}_{c(j)} = \mathscr{F}_{c(j)}^T \boldsymbol{l}_{c(j)}$ is the position vector of the origin of $\mathcal{F}_j$ relative to the origin of $\mathcal{F}_{c(j)}$.

4.2 Prismatic Joint

The prismatic joints are embedded in each strut. Active actuators, such as voice coil motors, are mounted in the prismatic joints to control the length of the struts, so that the attitude and position of the payload can be changed. When establishing the equations of motion of the system, the struts should be viewed as two connected rigid links. Denote the upper link by B_j and the lower link by $\mathrm{B}_{c(j)}$. The allowed translational velocity at the joint is

$$\dot{\vec{t}}_j = \mathscr{F}_j^T \dot{\boldsymbol{t}}_j = \mathscr{F}_j^T \boldsymbol{\Gamma}_j \boldsymbol{u}_j \tag{37}$$

where $\vec{t}_j$ is the translational displacement; $\vec{\Gamma}_j = \mathscr{F}_j^T \boldsymbol{\Gamma}_j$ is the vector signifying the direction of the displacement; $\boldsymbol{u}_j$ is the corresponding generalized speed.

Since there is no relative rotation between B_j and $\mathrm{B}_{c(j)}$, we have the following recursive relations,

$$\vec{\omega}_j = \vec{\omega}_{c(j)} = \boldsymbol{b}_{c(j)}^T \boldsymbol{\omega}_{c(j)}, \quad {}^p\vec{\omega}_j = {}^p\vec{\omega}_{c(j)}, \quad \dot{\vec{\omega}}_{jt} = \dot{\vec{\omega}}_{c(j)t} \tag{38}$$

Yet for the velocities, we have

$$\vec{v}_j = \mathscr{F}_{c(j)}^T \boldsymbol{v}_{c(j)} - \mathscr{F}_{c(j)}^T (\tilde{\boldsymbol{l}}_{c(j)} + \tilde{\boldsymbol{t}}_{hj}) \boldsymbol{\omega}_{c(j)} + \mathscr{F}_{c(j)}^T \dot{\boldsymbol{t}}_{hj} \tag{39}$$

Differentiating Eq. (39) with respect to time, the recursive relation of $\dot{\vec{v}}_{jt}$ can be obtained as

$$\dot{\vec{v}}_{jt} = \dot{\vec{v}}_{c(j)t} - \mathscr{F}_{c(j)}^T (\tilde{\boldsymbol{l}}_{c(j)} + \tilde{\boldsymbol{t}}_{hj}) \mathscr{F}_{c(j)} \dot{\vec{\omega}}_{c(j)t} + \mathscr{F}_{c(j)}^T \tilde{\boldsymbol{\omega}}_{c(j)} \tilde{\boldsymbol{\omega}}_{c(j)} (\boldsymbol{l}_{c(j)} + \boldsymbol{t}_{hj}) + 2\mathscr{F}_{c(j)}^T \tilde{\boldsymbol{\omega}}_{c(j)} \dot{\boldsymbol{t}}_{hj} \tag{40}$$

Substitute Eq. (13) into Eq. (39), we have

$${}^p\vec{v}_j = {}^p\vec{v}_{c(j)} - \mathscr{F}_{c(j)}^T (\tilde{\boldsymbol{l}}_{c(j)} + \tilde{\boldsymbol{t}}_{hj}) \mathscr{F}_{c(j)} {}^p\vec{\omega}_{c(j)} + \begin{bmatrix} \boldsymbol{0} & \cdots & \mathscr{F}_{c(j)}^T \boldsymbol{\Gamma}_{hj} & \cdots & \boldsymbol{0} \end{bmatrix} \tag{41}$$

4.3 Hooke Joint and Spherical Joint

The lower links are mounted on the central hub by Hooke joints, whereas the upper links are connected to the payload through spherical joints. These two joints have similar recursive kinematic relations as the revolute joint, but the definitions of $\vec{\Gamma}_j$ and $\boldsymbol{u}_j$ are different. The spherical joint permits the two adjacent bodies rotate in three DOFs. We adopt the Euler angles in "3-1-2" rotational sequence to describe the relative attitude. Thus we have

$$\boldsymbol{\Gamma}_j = \begin{bmatrix} \cos\theta & 0 & -\cos\phi\sin\theta \\ 0 & 1 & \sin\phi \\ \sin\theta & 0 & \cos\phi\cos\theta \end{bmatrix}, \quad \boldsymbol{u}_j = \dot{\Theta}_j \triangleq \begin{bmatrix} \dot{\phi} \\ \dot{\theta} \\ \dot{\psi} \end{bmatrix} \tag{42}$$

where ϕ, θ, and ψ are the three successive rotation angles. Compared with the revolute joint, $\boldsymbol{\Gamma}_j$ is also time varying, so it should be incorporated when formulating the recursive relations for the angular accelerations.

As for the Hooke joint, two successive rotation angles are defined to describe the relative attitude of the two connected bodies. If the "1-2" rotational sequence is used, we have

$$\boldsymbol{\Gamma}_j = \begin{bmatrix} \cos\varphi & 0 \\ 0 & 1 \\ \sin\varphi & 0 \end{bmatrix}, \quad \boldsymbol{u}_j = \dot{\Theta}_j \triangleq \begin{bmatrix} \dot{\theta} \\ \dot{\varphi} \end{bmatrix} \tag{43}$$

4.4 Generalized Speeds for the SMSS

Basing on the discussions above, the generalized speeds of the system $\boldsymbol{u}$ are specified in this sub-section. Following the body numbers in Fig. 2, the generalized speeds are defined in Table 1.

Table 1. System Generalized Speeds.

Generalized Speeds	Descriptions
$\boldsymbol{v}_1 \in \mathbb{R}^{3\times1}$	Inertial velocity of B1
$\boldsymbol{\omega}_1 \in \mathbb{R}^{3\times1}$	Inertial angular velocity of B1
$\dot{\boldsymbol{\Theta}}_j \in \mathbb{R}^{2\times1}$	Rotational speeds in Hooke joints. $j = 11, 21, 31, 41, 51, 61$
$\dot{\boldsymbol{t}}_j \in \mathbb{R}^{1\times1}$	Translational speeds in prismatic joints. $j = 12, 22, 32, 42, 52, 62$
$\boldsymbol{\omega}_{13} \in \mathbb{R}^{3\times1}$	The relative angular velocity at the spherical joint.

$\dot{\theta}_j$	Rotational speeds at the revolute joints connecting the solar panels. $j=71,81$
$\dot{\boldsymbol{\tau}}_j$	Modal coordinates for the flexible payload and the two solar panels. $j=13,71,81$

5. Motion Constraints

In this section, the motion constraints will be developed for the Stewart mechanism. To obtain the unconstrained system, we introduce five cut points at the spherical joints to eliminate the closed loop, which brings in 15 constraint equations.

Taking the constraint equation for Strut 2 (constituted of B21 and B22, as Fig. 2 shows) as an example, the constraint equations for other struts can be similarly obtained.

The motion constraint for the closed-loop is derived from a straightforward observation: the relative velocity between C22 and C23 is zero, where C22 and C23 are the cut points at B22 and the payload B13 respectively, as Fig. 5 demonstrated.

$$\vec{\boldsymbol{v}}_{C23}=\vec{\boldsymbol{v}}_{C22} \tag{44}$$

where $\vec{\boldsymbol{v}}_{C22}$ and $\vec{\boldsymbol{v}}_{C23}$ are the inertial velocity of C22 and C23, respectively.

It should be noted that, the payload is attached on the rigid upper platform of the Stewart mechanism, therefore, we do not have to consider the structural flexibility when establishing the constraint equations.

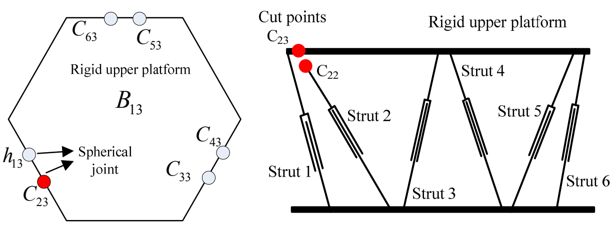

Fig. 4 The rigid upper platform of the Stewart.

Expanding Eq. (44) by the system generalized speeds, we have

$$\boldsymbol{C}_{11}\boldsymbol{\Gamma}_{11}\dot{\boldsymbol{\Theta}}_{11}+\boldsymbol{C}_{12}\boldsymbol{\Gamma}_{12}\dot{t}_{12}+\boldsymbol{C}_{13}\boldsymbol{\omega}_{13}=\boldsymbol{C}_{21}\boldsymbol{\Gamma}_{21}\dot{\boldsymbol{\Theta}}_{21}+\boldsymbol{C}_{22}\boldsymbol{\Gamma}_{22}\dot{t}_{22} \tag{45}$$

where $\boldsymbol{\Gamma}_j(j=11,12,21,22)$ are the vectors characterizing the direction of motion for each joints. They are defined in Eqs. (37), (42) and (43). $\boldsymbol{C}_j(j=11,12,13,21,22)$ are the coefficient matrices determined by the system configuration.

The generalized speeds in Eq. (45) can be divided into two parts: the dependent ones $\boldsymbol{u}_{D,2}$ and the independent ones $\boldsymbol{u}_I$. Then we have

$$\boldsymbol{u}_{D,2}=[\dot{\boldsymbol{\Theta}}_{h21}{}^T,\dot{t}_{h22}]^T\in\mathbb{R}^{3\times1},\ \boldsymbol{u}_I=[\dot{\boldsymbol{\Theta}}_{h11}{}^T,\dot{t}_{h12},\boldsymbol{\omega}_{h13}{}^T]^T\in\mathbb{R}^{6\times1} \tag{46}$$

Then the constraint equation for Strut 2 is written as

$$\boldsymbol{G}_{1,2}\boldsymbol{u}_{D,2}=\boldsymbol{G}_{2,2}\boldsymbol{u}_I \tag{47}$$

where

$$\boldsymbol{G}_{1,2}=[\boldsymbol{C}_{21}\boldsymbol{\Gamma}_{21},\boldsymbol{C}_{22}\boldsymbol{\Gamma}_{22}]\in\mathbb{R}^{3\times3}$$
$$\boldsymbol{G}_{2,2}=[\boldsymbol{C}_{11}\boldsymbol{\Gamma}_{11},\boldsymbol{C}_{12}\boldsymbol{\Gamma}_{12},\boldsymbol{C}_{13}]\in\mathbb{R}^{3\times6} \tag{48}$$

The constraints equations for Struts 3-6 can be obtained by following the derivation in Eqs. (44)-(48). Thus, all of the constraints equations are gathered to form

$$\boldsymbol{G}_1\boldsymbol{u}_D=\boldsymbol{G}_2\boldsymbol{u}_I \tag{49}$$

where

$$\boldsymbol{G}_1=\begin{bmatrix}\boldsymbol{G}_{1,2}&&&&\\&\boldsymbol{G}_{1,3}&&&\\&&\boldsymbol{G}_{1,4}&&\\&&&\boldsymbol{G}_{1,5}&\\&&&&\boldsymbol{G}_{1,6}\end{bmatrix}\in\mathbb{R}^{15\times15}$$

$$\boldsymbol{G}_2=\begin{bmatrix}\boldsymbol{G}_{2,2}\\\boldsymbol{G}_{2,3}\\\boldsymbol{G}_{2,4}\\\boldsymbol{G}_{2,5}\\\boldsymbol{G}_{2,6}\end{bmatrix}\in\mathbb{R}^{15\times3},\quad \boldsymbol{u}_D=\begin{bmatrix}\boldsymbol{u}_{D,2}\\\boldsymbol{u}_{D,3}\\\boldsymbol{u}_{D,4}\\\boldsymbol{u}_{D,5}\\\boldsymbol{u}_{D,6}\end{bmatrix}\in\mathbb{R}^{15\times1} \tag{50}$$

Equation (49) stands for the motion constraints in the Stewart mechanism. It will be combined with the equations of motion of the unconstrained system in Eq. (28) to describe the complete dynamic model of the multi-pointing stewart system in Fig. 2.

6. Application of the New Form of Kane's Equation

In this section, the new form of Kane's equation is adopted to form the equations of motion without introducing unknown multipliers, so that the resultant model is suitable for controller design.

Divide the generalized speeds in Table 1 into three groups as

$$\boldsymbol{u}=[\boldsymbol{u}_0^T,\boldsymbol{u}_I^T,\boldsymbol{u}_D^T]^T \tag{51}$$

where $\boldsymbol{u}_I$ and $\boldsymbol{u}_D$ are given in Eq. (47) and (50). $\boldsymbol{u}_0$ is the generalized speeds irrelevant to the motion constraints:

$$\boldsymbol{u}_0=[\boldsymbol{v}_1^T,\boldsymbol{\omega}_1^T,\dot{\theta}_{71},\dot{\theta}_{81},\dot{\boldsymbol{\tau}}_{13}^T,\dot{\boldsymbol{\tau}}_{71}^T,\dot{\boldsymbol{\tau}}_{81}^T]^T \tag{52}$$

Then, the equations of motion in Eq. (28) should be rearranged and also be divided into three parts:

$$\begin{bmatrix}\boldsymbol{M}_0\\\boldsymbol{M}_I\\\boldsymbol{M}_D\end{bmatrix}\begin{bmatrix}\dot{\boldsymbol{u}}_0\\\dot{\boldsymbol{u}}_I\\\dot{\boldsymbol{u}}_D\end{bmatrix}+\begin{bmatrix}\boldsymbol{F}_{t0}^I\\\boldsymbol{F}_{tI}^I\\\boldsymbol{F}_{tD}^I\end{bmatrix}=\begin{bmatrix}\boldsymbol{F}_0^A\\\boldsymbol{F}_I^A\\\boldsymbol{F}_D^A\end{bmatrix} \tag{53}$$

Transform Eq. (49) into the standard constraint equation as

$$\boldsymbol{u}_D=\boldsymbol{A}\boldsymbol{u}_I \tag{54}$$

where $\boldsymbol{A}=\boldsymbol{G}_1^{-1}\boldsymbol{G}_2$. Differentiating Eq. (54) with respect to time leads to the constraint equations in acceleration level:

$$\boldsymbol{A}_1\begin{bmatrix}\dot{\boldsymbol{u}}_I\\\dot{\boldsymbol{u}}_D\end{bmatrix}=\dot{\boldsymbol{A}}\boldsymbol{u}_I \tag{55}$$

where $\boldsymbol{A}_1\triangleq[-\boldsymbol{A}\ \ \boldsymbol{I}]$. According to Ref. 10), we define the orthogonal complements matrix of $\boldsymbol{A}_1$ as $\boldsymbol{A}_2=[\boldsymbol{I}\ \ \boldsymbol{A}^T]$. Thus Eq. (53) can be projected by $\boldsymbol{A}_2$ as

$$\begin{bmatrix}\boldsymbol{M}_0\\\boldsymbol{A}_2\begin{bmatrix}\boldsymbol{M}_I\\\boldsymbol{M}_D\end{bmatrix}\\[\boldsymbol{0}\ ,\ \boldsymbol{A}_1]\end{bmatrix}\begin{bmatrix}\dot{\boldsymbol{u}}_0\\\dot{\boldsymbol{u}}_I\\\dot{\boldsymbol{u}}_D\end{bmatrix}+\begin{bmatrix}\boldsymbol{F}_{t0}^I\\\boldsymbol{A}_2\begin{bmatrix}\boldsymbol{F}_{tI}^I\\\boldsymbol{F}_{tD}^I\end{bmatrix}\\\dot{\boldsymbol{A}}\boldsymbol{u}_I\end{bmatrix}=\begin{bmatrix}\boldsymbol{F}_0^A\\\boldsymbol{A}_2\begin{bmatrix}\boldsymbol{F}_I^A\\\boldsymbol{F}_D^A\end{bmatrix}\\\boldsymbol{0}\end{bmatrix} \tag{56}$$

From Eq. (56) we can see that the equations of motion are composed of three parts:

Firstly,

$$M_0\dot{u}_0 + F_{t0}^I = F_0^A ,$$

which is the equations of motion for the generalized speeds $\dot{u}_I$.

Secondly,

$$A_2\begin{bmatrix} M_I \\ M_D \end{bmatrix}\dot{u}_I + A_2\begin{bmatrix} F_{tI}^I \\ F_{tD}^I \end{bmatrix} = A_2\begin{bmatrix} F_I^A \\ F_D^A \end{bmatrix},$$

which is the reduced equations of motion for u_I and u_D. The dimension of this equation is same as u_I .

Thirdly,

$$A_1\begin{bmatrix} \dot{u}_I \\ \dot{u}_D \end{bmatrix} = \dot{A}u_I ,$$

which is the constraint equation.

It is obvious that the equations above are free of multipliers and has the same dimension with the system generalized speeds. However, it should be noted that, the constraint equations at the acceleration level should be twice integrated to obtain the generalized coordinates. It makes the numerical solutions sensitive to the finite precision and accuracy errors.

Therefore, we have to utilize certain approaches, such as the Baumgarte's constraint violation stabilization technique,[13,14] for constraint enforcement while numerically integrating Eq. (56).

Observing Eq. (56), we find that the new form of Kane's equation belongs to the common projective methods for constrained multibody systems.[15] The key feature of this method is that the projection matrix $A_2 = [I \;\; A^T]$ is directly constructed by the coefficient matrix A in the constraint equation $u_D = Au_I$. A rigorous formulation can be found in Ref. 10) for more details.

Furthermore, noting that $\begin{bmatrix} u_I^T & u_D^T \end{bmatrix}^T = A_2 u_I$, we further reduce the first two parts in Eq. (56) to

$$\begin{bmatrix} M_0 & \\ & A_2\begin{bmatrix} M_I \\ M_D \end{bmatrix}A_2 \end{bmatrix}\begin{bmatrix} \dot{u}_0 \\ \dot{u}_I \end{bmatrix} + \begin{bmatrix} F_{t0}^I \\ A_2\left(\begin{bmatrix} F_{tI}^I \\ F_{tD}^I \end{bmatrix} + \dot{A}_2 u_I\right) \end{bmatrix} = \begin{bmatrix} F_0^A \\ A_2\begin{bmatrix} F_I^A \\ F_D^A \end{bmatrix} \end{bmatrix} \quad (57)$$

Equation (57) is only related to the independent generalized speeds. The dependent one $\dot{u}_D$ can be solved from the third part of Eq. (56), which means that the control synthesis could be directly performed on Eq. (57). However, not all the joints are embedded with active actuators. Consequently, the designed control, expressed as

$$F_{design}^A = A_2\begin{bmatrix} F_I^A \\ F_D^A \end{bmatrix},$$

is actually the projection of the real control on the subspace of the independent variables. To solve this problem, the following weighted pseudo-inversion logic is employed for the redistribution of the control input,

$$\begin{bmatrix} F_I^A \\ F_D^A \end{bmatrix} = WA_2^T(A_2WA_2^T)^{-1}A_2F_{design}^A \quad (58)$$

where $W = \mathrm{diag}[w_1,...,w_n] \in \mathbb{R}^{n\times n}$ is the weighted matrix. It needs to be emphasized that the w_i corresponding to the Hooke joints and spherical joints should be zero, since no actuators are located in those joints.

7. Numerical Simulations

In this section, the dynamic model of the SMSS established by the proposed methodology is compared with the simplified model in which the struts are considered as a group of spring damper without mass.[4]

The mass properties of the considered system is given in Table 2. The exciting torques in the central hub and the active forces in the struts are given in Table 3.

Table 2. Mass properties.

Items	Values
Mass of the rigid hub	2000kg
Mass of the upper platform and payload	1000kg
Moment of inertia of the rigid hub	diag(1000,1000,800) $\mathrm{kg\cdot m^2}$
Moment of inertia of the upper platform and payload	diag(500,500,250) $\mathrm{kg\cdot m^2}$

Table 3. Exciting torques and active forces.

Items	Values
Exciting torques in central hub	[1 1 1] $\mathrm{N\cdot m}$
Active forces in Struts 1 to 6	0.1N

By inserting the same forces in to the two models, we presented a 10s simulation. The time histories of Euler angle of the central hub and the upper platform solved by the two model are compared in Figs. 5 and 6 respectively. As we can see, the responses of the central hub and the upper platform solved by the two models are consistent.

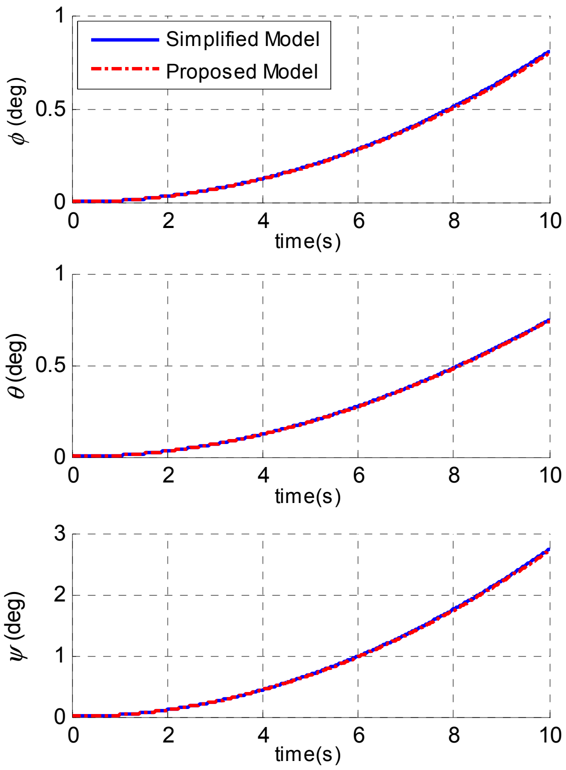

Fig. 5. Euler angles of the rigid hub by two models (deg).

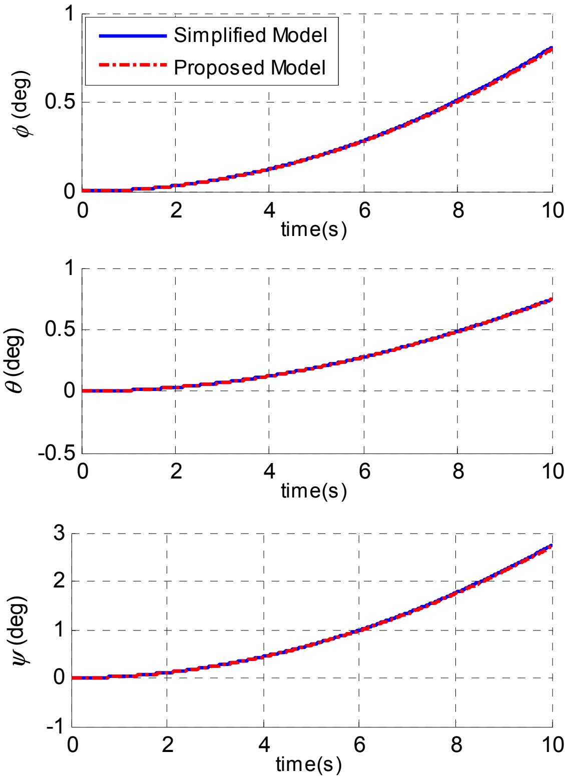

Fig. 6. Euler angles of the upper platform (deg).

The error of length of each strut between the two models are given in Fig. 7. Its order of magnitude is 10^{-6}m, which means the error of struts' deformation between the two models are rather small. Thus, the results of the two model agree with each other.

It should be noted that, since we assume that the mass and inertia of the payload are comparable with the rigid hub, both of which are much bigger than the mass and inertia of the Stewart mechanism, so the results of the two model agree well. However, when the inertia is comparable with the Stewart, the proposed model should be used. Moreover, another advantage of the proposed method is that the flexibility of the payload and the flexible appendages can be described.

8. Conclusions

In this work, the detailed dynamics of the SMSS were formulated. A universal Kane's method in matrix form was developed first. It can be used for establishing the equations of motion of an arbitrary multibody system in tree topology. It permits that the body is rigid or flexible, and the joints connecting the bodies has 1~6 degrees of freedom. Then, the new form of Kane's method was combined with the Kane's method in matrix form to handle the motions constraints.

The proposed methodology was applied to a typical SMSS. The closed-loop constraints in the Stewart mechanism was first released, then the equations of motion for the unconstrained SMSS as well as the constraint equations were derived and combined.

A numerical example shows that the dynamic model established by the methodology above is in correspondence with the pre-existing model. The obtained equations of motion are free of multipliers, thus would be more suitable for control synthesis.

Future work will be focused on the controller design and specific applications of SMSS.

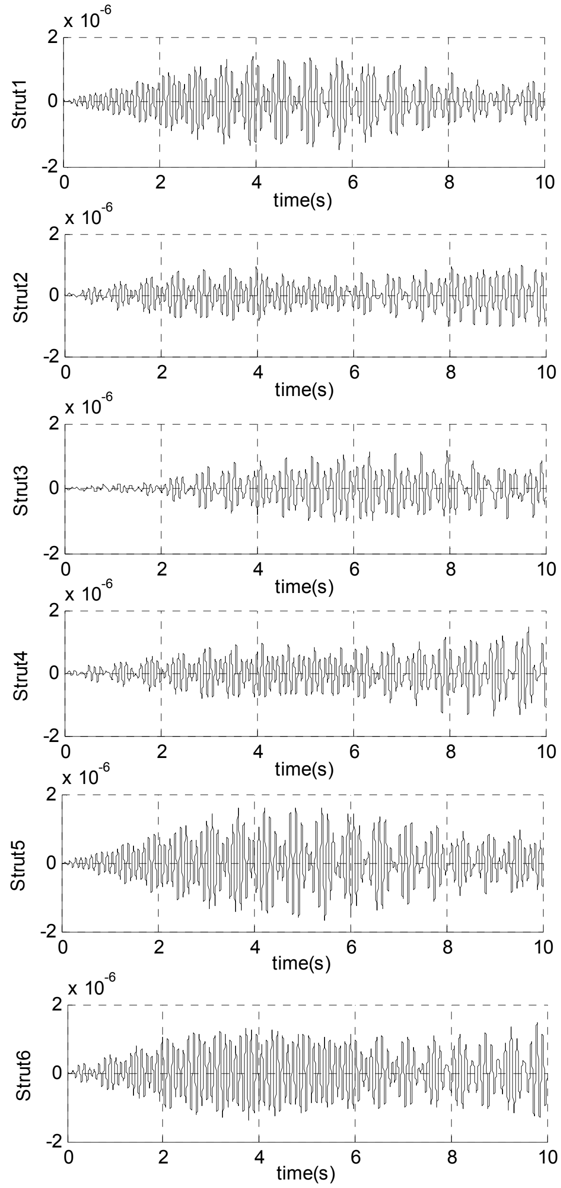

Fig. 7. Error of the struts' length (m).

Acknowledgments

This paper reports work carried out in the project supported by the National Natural Science Foundation of China (11502018) and the Seed Foundation of Qian Xuesen Laboratory of Space Technology.

Appendix: Integrals in Eq. (21)

$m_j = \int_{Bj} dm$ is the mass of B_j.

$\vec{S}_j = \int_{Bj}(\vec{r}_{mj} + \vec{u}_{mj})dm \approx \int_{Bj}\vec{r}_{mj}dm$ is the first moment of inertia of B_j.

$\vec{J}_j = \int_{Bj}[(\vec{r}_{mj} + \vec{u}_{mj})\cdot(\vec{r}_{mj} + \vec{u}_{mj})\boldsymbol{I}_3 - (\vec{r}_{mj} + \vec{u}_{mj})(\vec{r}_{mj} + \vec{u}_{mj})]dm$

$\approx \int_{Bj}[\vec{r}_{mj}\cdot\vec{r}_{mj}\boldsymbol{I}_3 - \vec{r}_{mj}\vec{r}_{mj}]dm$ is the second moment of inertia.

$\vec{P}_j = \int_{Bj}\vec{T}_{mj}dm$ is the modal momentum coefficient.

$\vec{H}_j = \int_{Bj}(\vec{r}_{mj} + \vec{u}_{mj})\times\vec{T}_{mj}dm \approx \int_{Bj}\vec{r}_{mj}\times\vec{T}_{mj}dm$ is the modal angular momentum coefficient.

$\boldsymbol{E}_j = \int_{Bj}\vec{T}_{mj}\cdot\vec{T}_{mj}dm$ is the modal mass of B_j. If normal modes are utilized, $\boldsymbol{E}_j$ is an unity matrix.

$\vec{H}_{\omega j}$, $\vec{F}_{\omega j}$, and $\vec{F}_{\omega\omega j}$ are nonlinear terms given by,

$$\vec{H}_{\omega j} = \int_{Bj}(\vec{r}_{mj} + \vec{u}_{mj})\times(\vec{\omega}_j\times\vec{T}_{mj})dm \approx \int_{Bj}\vec{r}_{mj}\times(\vec{\omega}_j\times\vec{T}_{mj})dm$$

$$\vec{F}_{\omega j} = \int_{Bj}\vec{T}_{mj}\cdot(\vec{\omega}_j\times\vec{T}_{mj})dm$$

$$\vec{F}_{\omega\omega j} = \int_{Bj}\vec{T}_{mj}\cdot(\vec{\omega}_j\times(\vec{\omega}_j\times(\vec{r}_{mj} + \vec{u}_{mj})))dm$$

$$\approx \int_{Bj}\vec{T}_{mj}\cdot(\vec{\omega}_j\times(\vec{\omega}_j\times\vec{r}_{mj}))dm$$

References

1) Pittens, K. H. and Podhorodeski, R. P.: A family of stewart platforms with optimal dexterity, *Journal of Robotic Systems*, **10**(1993), pp. 463–479.
2) John, J. F., Mcinroy, O. E., and Neat, G. W.: Pracise, Fault-Tolerence Pointing Using a Stewart Platform, *IEEE/ASME Transactions on Mechatronics*, **4**(1999), pp. 91–95.
3) Liu, M., Li, C., and Li, C.: Dynamics Analysis of the Gough -Stewart Platform Manipulator, *IEEE Transactions on Robotics and Automation*, **16**(2000), pp. 94–98.
4) Zhang, Y., Zhang, J., Zhai, G., et.al. : High imaging performance of optical payload by vibration isolation system, AIAA Guidance, Navigation, and Control Conference, Aug., 2012.
5) Zhang, Y. and Zhang, J.: Disturbance characteristics analysis of CMG due to imbalances and installation errors, *IEEE Transactions on Aerospace and Electronic Systems*, **50**(2014), pp. 1017–1026.
6) Zhang, Y., Li, M., Song, Z., Shan, J., Guan, X. and Tang, L.: Design and analysis of a moment control unit for agile satellite with high attitude stability requirement, *Acta Astronautica*, **122**(2016), pp. 90–105.
7) Geng, Z., Haynes, L. S., Lee, J. D. and Carroll, R. L.: On the dynamic model and kinematic analysis of a class of stewart platforms. *Robotics & Autonomous Systems*, **9**(4), pp. 237-254.
8) Dasgupta, B. and Mruthyunjaya, T. S.: Closed-Form Dynamic Equations of the General Stewart Platform through the Newton–Euler Approach, *Mechanism and Machine Theory*, **33**(1998), pp. 993–1012.
9) Dasgupta, B. and Mruthyunjaya, T. S.: A Newton-Euler formulation for the inverse dynamics of the Stewart platform manipulator, *Mechanism and Machine Theory*, **33**(1998), pp. 1135–1152.
10) Bajodah, A. H., Hodges, D. H. and Chen, Y. H.: New Form of Kane's Equations of Motion for Constrained Systems, *Journal of Guidance, Control, and Dynamics*, **26**(2003), pp. 79–88.
11) Banerjee, A. K. and Kane, T. R: Large motion dynamics of a spacecraft with a closed-loop, articulated, flexible appendage, 25th AIAA/ASME Structures, Structural Dynamics and Materials Conference, May, 1984.
12) Hu, Q., Jia, Y. and Xu, S.: A new computer-oriented approach with efficient variables for multibody dynamics with motion constraints, *Acta Astronautica*, **81**(2012), pp. 380–389.
13) Yoon, S., Howe, R. M. and Greenwood, D.T.: Stability and Accuracy Analysis of Baumgarte's Constraint Violation Stabilization Method, *Journal of Mechanical Design*, **117**(1995), pp. 446–453.
14) Bauchau, O. A., and Laulusa, A.: Review of Contemporary Approaches for Constraint Enforcement in Multibody Systems, *Journal of Computational and Nonlinear Dynamics*, **3**(2008), pp. 011005.
15) Borri, M., Bottasso, C. L. and Mantegazza, P.: Acceleration Projection Method in Multibody Dynamics, Eur. J. Mech. A/Solids, **11**(1992), pp. 403–418.